Real data estimation of crosswell seismic radiation pattern for a fluid-coupled piezoelectric source and hydrophone receivers

James W. Rector*, *University of California, Berkeley;* and Spyros K. Lazaratos, *TomoSeis, Inc.*

BG5.3

Summary

Cross-well seismic imaging has been evolving from techniques using only traveltimes (such as traveltime tomography) to techniques more akin to VSP and surface seismic data that utilize reflections and other scattered energy. In order to properly image cross-well data with accurate amplitude information it is necessary to understand the radiation patterns of cross-well seismic sources and receivers. In this paper we apply the extensive theoretical developments in fluid-coupled source and receiver modeling to real cross-well data recorded in West Texas. Theory predicts that the amplitudes of cross-well arrivals are extremely dependent upon the formation velocities adjacent to the source and receiver wells. Direct arrival amplitudes can vary by a factor of 1,000 in the same cross-well survey. The theory closely resembles what is seen in real data recorded in West Texas after incorporating propagation effects.

To obtain true amplitude information from cross-well reflection images obtained with fluid-coupled sources and receivers, the near borehole environment (borehole radius, casing, cement thickness, and formation velocity/density) should be well characterized. Conversely, the strong sensitivity of cross-well amplitudes to formation properties suggest that amplitude information from cross-hole surveys may reveal a great deal about the formation properties near the borehole.

Introduction

Although there have been many papers dealing with the wavefield modeling of borehole sources and hydrophone receivers, there have been few published studies relating to field analysis of the amplitude and radiation/reception patterns of downhole sources and receivers. The lack of field study is primarily due to the fact that, up until recently, most analysis of real cross-well data sets consisted of producing traveltime tomograms and arrival amplitudes were of secondary importance.

Recently, it has been recognized (Williamson and Worthington, 1993, Rector and Washbourne, 1994) that traveltime tomography does not have sufficient resolution to image small heterogeneities (less than 5 m) at standard oil and gas well spacings (40 to 160 acres). Consequently, more research emphasis has been placed on developing reflection imaging techniques using the reflected arrivals and diffraction tomography algorithms. Interestingly, although both theory and qualitative analysis of real data have indicated a significant change in body wave amplitude with angle and with formation impedance, some of the imaging algorithms do not incorporate these amplitude effects.

In this paper we use real cross-well seismic data from fluid-coupled sources and receivers acquired in West Texas (Harris, et al, 1992) to examine the combined radiation pattern of a piezoelectric bender source and hydrophone receivers. We also analyze the effect produced by the mechanical properties of the formation adjacent to the wellbore on the radiated and received energy.

Theory

The radiation pattern of seismic sources in open and cased boreholes has been investigated in several important papers (Lee and Balch, 1982, Winbow, 1991, and Peng et al, 1993). In the oil field environment of West Texas, which consists primarily of carbonate rocks and cased boreholes, the theoretical far field P-wave reception pattern of an omnidirectional hydrophone receiver centered in a fluid filled borehole (Peng, et al, 1993) can be approximated as:

$$M_\alpha = K_\alpha[1.3-\cos^2\delta], \qquad K_\alpha = \omega K/\rho\alpha\beta^2. \tag{1}$$

Likewise, the SV-wave reception pattern can be approximated as:

$$M_\beta = K_\beta[\sin 2\delta/(1-0.25\cos^2\delta)], \qquad K_\beta = \omega K/\rho\beta^3. \tag{2}$$

In the preceding expressions the transmission effects (divergence, layers, and Q) have been ignored and the terminology of Winbow (1991) has been used for the variables. The constant, K, stands for terms that are not angle or formation dependent. Assuming that the piezoelectric source can be also be approximated as a volume change, equations 1 and 2 also describe the radiation pattern of the piezoelectric source in West Texas carbonates.

For our purposes, the important features of equations 1 and 2 are:

1) Ignoring the angle dependence, the magnitude of the radiated/received energy varies strongly with the formation parameters adjacent to the wellbore--as $1/\rho\alpha\beta^2$ for the P-wave and as $1/\rho\beta^3$ for the SV-wave. Consequently, the combined effects of source and receiver radiation in carbonate rocks, where the density, ρ, can vary by 10% and the velocity, α or β, can vary by 50%, should theoretically produce body-wave amplitude differences in the same cross-well survey of *1 to 2 orders of magnitude*. In more simple terms, the cross-well arrivals radiated and received at one depth can be yp to *100 times less* than the cross-well arrivals radiated and received at another depth *without* considering transmission, spreading, Q or radiation pattern.

2) The angle dependent effects of the radiation pattern are not strongly formation dependent since Poission's ratio can be considered as roughly constant in many carbonates.

Angle Dependence in Real Cross-Well Data

The Mcelroy cross-well data described by Harris et al (1992) is an ideal test site for measuring the radiation pattern in carbonates because Poisson's ratio was nearly constant with depth, the survey aperture (about 67 degrees from the horizontal) was large compared to the well spacing (184 ft (56 m)), and the wells were nearly vertical. Figure 1 shows the acquisition geometry employed at the Mcelroy site. Source and receiver positions were recorded at 2.5 ft (.76m) intervals over a 500 ft (153m) vertical aperture between 2650 and 3150 ft. The axes in Figure 1 are referenced to a datum that is 1,000 ft (306 m below the ground level at the site). Using equations 1 and 2, we computed a theoretical curve combining of the average hydrophone reception pattern and the piezoelectric source radiation pattern at the Mcelroy field site. The average P-wave formation velocity, α, from the P-wave tomogram

(Van Schaack et al, 1992) was 4970 m/s and the average S-wave velocity, β, was assumed to be 2980 m/s, producing a Poission's ratio, ν, of 0.24.

To investigate the applicability of this theoretical radiation pattern to real data, we computed the average P-wave and SV-wave direct arrival amplitude as a function of offset (defined as the vertical distance between source and receiver) for the Mcelroy cross-well data set. We computed the average direct arrival amplitude by first picking and aligning the direct arrival and then stacking the data from each offset. By stacking the data for each offset we hoped to average out the effects of raybending, transmission, changes in poisson's ratio, changes in rock impedance, and interference from other arrivals (reflection, conversions, guided waves, etc). Figure 2 shows the P-wave direct arrival aligned to a time of 5 ms. Figure 2 also shows rms amplitude estimated from a 6 ms window around the direct arrival along with the theoretical radiation pattern. To incorporate both source and receiver effects, the theoretical radiation pattern represents the square of the angle dependent term in equation 1. Attenuation due to geometric spreading was removed assuming straight raypaths before computing the amplitudes. Note that the P-wave radiation pattern closely approximates theory at the more vertical raypaths, but deviates substantially from theory for the horizontal raypaths.

We believe that the near-horizontal raypath amplitudes for the P-wave direct arrival deviate from theory because of transmission and raybending effects caused by the horizontal layering of the earth at this location. The 'nearly' horizontal raypaths are more attenuated than vertical raypaths due to the (generally) smaller transmission coefficients at wider incidence angles. When the raypath becomes truly horizontal in horizontally-layered rocks, there are no transmission effects and the amplitude should dramatically increase. The effects of layering will be frequency dependent. The low frequency energy has a larger Fresnel Zone (Williamson and Worthington, 1993) and does not 'see' small scale layering. Therefore, we would expect a broader, less focused radiation/reception pattern for the lower frequencies. Figure 3 shows the amplitude versus angle display equivalent to Figure 3 except that the aligned and stacked data of Figure 2 were first frequency filtered from 300 to 1000 Hz (producing a Fresnel Zone of about 20 m). The radiation pattern in Figure 3 is much broader that the wideband radiation pattern shown in Figure 2.

To describe the effects of transmission and spreading at all frequencies we raytraced (and applied Zoeppritz equations at layer boundaries) through a 1-D layered P-wave velocity model produced through a constrained traveltime inversion. We then applied the same aligning and stacking procedure to the modeled data that we applied to the real data. Figure 4 shows the computed amplitude versus angle plot for the modeled data and the modeled radiation pattern including layer boundary transmission effects. Note that the peak in the radiation pattern at zero offset and the decrease in amplitude at higher offset is correctly predicted by the raytrace modeling. The corrected radiation pattern closely matches theory.

Figure 5 shows the radiation pattern for the SV-wave direct arrival computed in a similar manner. As expected there is a large null at horizontal angles and a maximum at about 40 degrees. The theoretical and measured radiation patterns are in close agreement.

The average ratio of maximum P-wave to maximum SV-wave direct arrival is about 2 to 1. Theory would predict a value of about 1 to 3. The six-fold difference between these amplitudes can probably be explained by Q. Also supporting the influence of Q is the frequency dependence of the P and SV-wave amplitudes. At a center frequency of 1,200 Hz, the amplitude of the P and S direct arrival energy roughly twice the amplitude at a center frequency of 600 Hz. Without the effects of Q, the product of equations 1 and 2, which is proportional to ω^2, would predict a factor of 4.

Formation Impedance Effects

To characterize the effects of formation impedance on the radiation and reception of P and SV energy we stacked the P-direct aligned data over a range of small vertical source/receiver offsets (-3 m to +3m). The rms amplitude was computed as before and then smoothed over 7m. Figure 6 shows the data, the smoothed RMS amplitudes, and the P and S velocities as computed from the cross-well traveltimes and the receiver well sonic logs. The maximum variation in the smoothed log data is about 30%, which when raised to the 6^{th} power, should produce a ratio of maximum to minimum amplitude of about 10 to 1. The smoothed amplitudes in Figure 6 vary by a factor of 10. The amplitudes shown in Figure 6 qualitatively agree with the logs. The low velocity reservoir interval centered at 2900 ft (886 m) is the zone of maximum amplitude. It appears that if a 30 ft static were applied to the logs, the amplitude changes would correlate very well with the logs. A quantitative relationship between the amplitudes and the logs may be difficult to obtain due to propagation effects. The amplitude of the direct arrival at small offsets would be expected to be larger where focusing of raypaths occurs and small in zones of lateral heterogeneities. Interestingly, the zone of low amplitude above 2750 ft (840 m) that does not correlate well with the logs is a zone of significant lateral heterogeneity (Lazaratos et al , 1992).

Conclusions and Implications

Theoretical work by Peng, et al (1993) accurately predicts the radiation and reception patterns of the fluid-coupled piezoelectric source and hydrophone receiver in West Texas Carbonates provided that Zoeppritz-related transmission effects are compensated at small offsets. Without Zoeppritz compensation, we observed an anomalously small P-wave direct arrival for an angular range from approximately 6 degrees to 17 degrees from the horizontal. The effect of layering is very sensitive to the frequency of the data. Lower frequency energy produced a less focused radiation pattern, one that did not require substantial compensation.

The P-wave direct arrival amplitude varies by a factor of 20 over a depth range of 500 ft (150m). This variation is in qualitative agreement with the variation observed in the logs and is comparable to the theoretical variation in amplitude, which predicts a value that is inversely proportional to $\alpha^2\beta^4$.

The dramatic effects of radiation pattern and formation impedance effects should be accounted for in doing any type of full-waveform imaging that incorporates amplitude information.

References

Harris, J.M., Nolen-Hoeksema, R., Rector, J.W., Lazaratos, S.K., and Van Schaack, M., "High Resolution Imaging of a West Texas Carbonate Reservoir: Part 1 Overview.", *Presented at the 62nd Ann. Mtg. of SEG*, New Orleans. Expanded Abstracts, 35-38

Lazaratos, S.K., Rector, J.W., Van Schaack, M., Harris, J.M.," High Resolution Imaging of a West Texas Carbonate Reservoir: Part 4 Reflection Imaging"., *Presented at the 62nd Ann. Mtg. of SEG*, New Orleans. Expanded Abstracts 49-53.

Lee, M.W., and Balch, A.H., 1982, Theoretical seismic wave radiation from a fluid filled borehole, Geophysics, 47, 1308-1314.

Peng, C., Cheng, C.H., and Toksoz, M.N., 1993, Cased borehole effects on downhole seismic measurements; Extended Abstracts C054, EAEG 55th Ann. Mtng., Stavanger, Norway.

Rector, J.W., and Washbourne, J., 1994, Characterization of resolution and uniqueness in cross-well direct arrival traveltime tomography using the fourier projection slice theorem, Geophysics, in press.

Van Schaack, M., Harris, J.M., Rector, J.W., and Lazaratos, S.K., "High Resolution Imaging of a West Texas Carbonate Reservoir: Part 2 Traveltime Tomography", *Presented at the 62nd Ann. Mtg. of SEG*, New Orleans. Expanded Abstracts, 40-44.

Williamson, P. R., and Worthington, M. H., 1993, Resolution limits in ray tomography due to wave behavior: numerical experiments, Geophysics, 58.5, 727-736

Winbow, G.A., 1991, Seismic sources in open and cased boreholes, Geophysics,56,1040-1050.

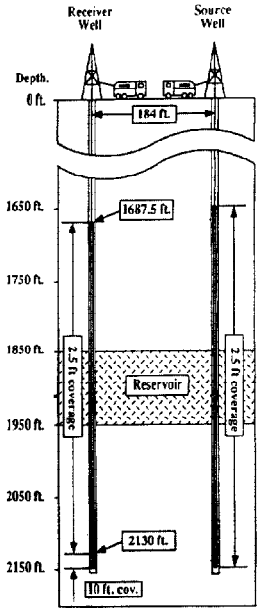

Figure 1 (taken from Van Schaack, et al. 1992): Acquisition Geometry used at Mcelroy field site.

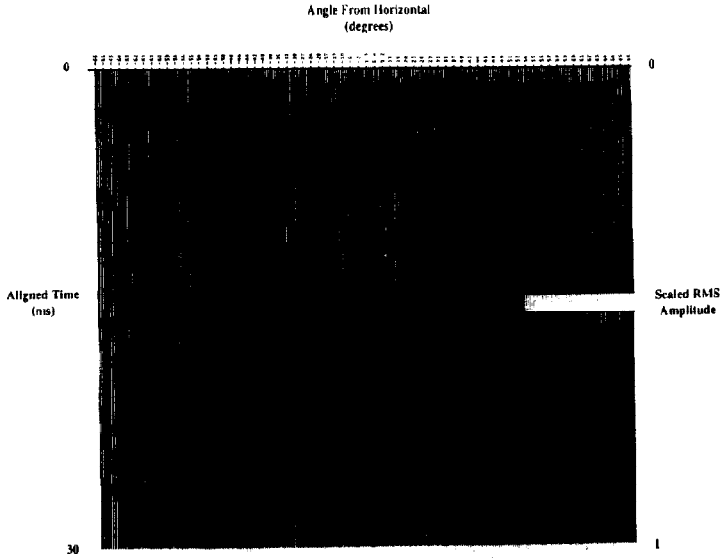

Figure 2: Scaled RMS amplitude of the P-wave direct arrival (dark curve) and theoretical combined radiation pattern of the piezoelectric source and the hydrophone receiver (light curve), superimposed on P-direct aligned and stacked data.

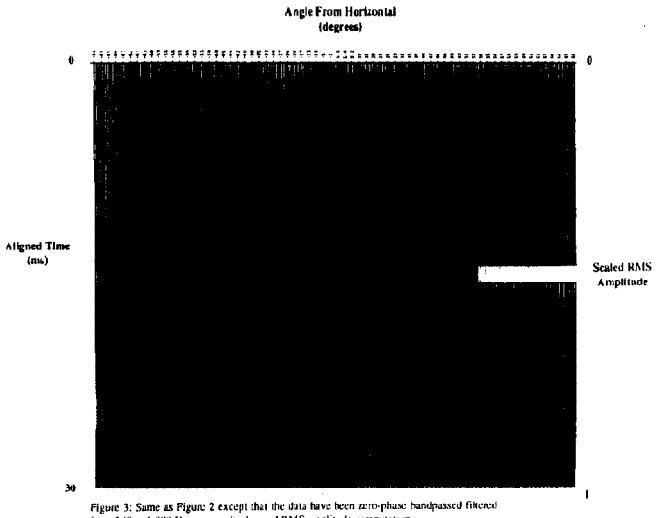

Figure 3: Same as Figure 2 except that the data have been zero-phase bandpassed filtered from 300 to 1,000 Hz prior to display and RMS amplitude computation.

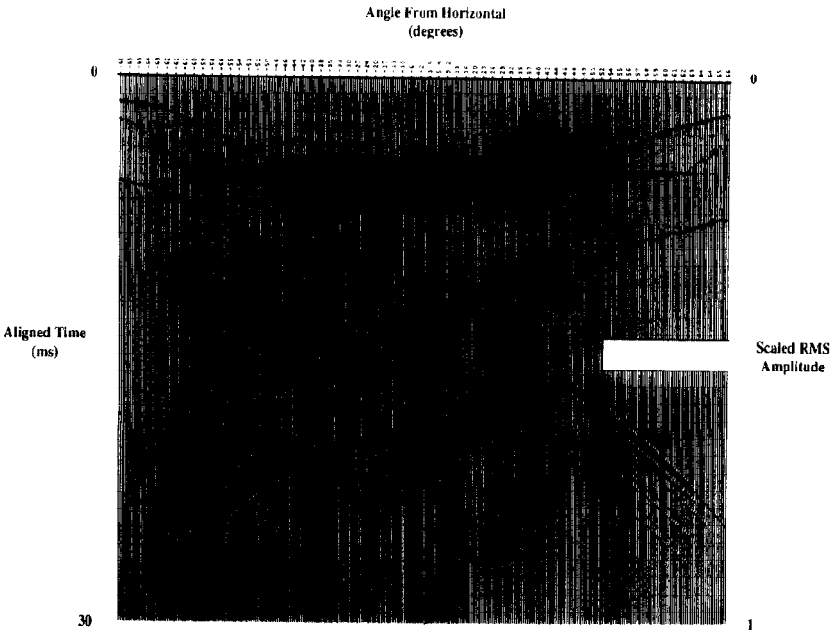

Figure 4: Same as Figure 2 except light curve is scaled RMS amplitude of P wave direct arrival and darker curves are a) modeled effects of transmission through layers (the smaller amplitude curve) and b) combined effects of transmission and radiation/reception.

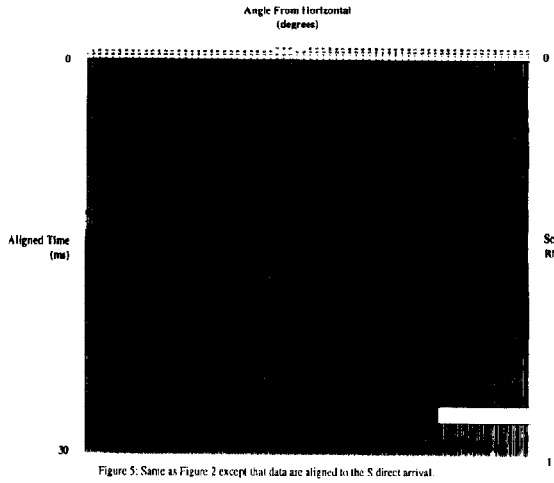

Figure 5: Same as Figure 2 except that data are aligned to the S direct arrival.

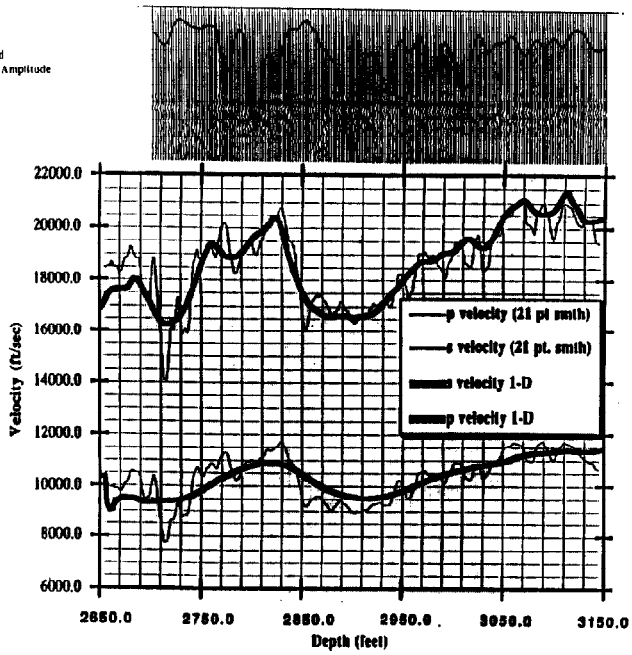

Figure 6: Smoothed velocity data as a function of depth (taken from Van Schaack, et al, 1992) and RMS amplitude of stacked near offset (-10 ft to +10 ft from horizontal) data. The time axis goes from 0 to 10 ms, and the scaled RMS amplitudes range from 0 to 1.